Use of Constrained Synthetic Amino Acids in β-Helix Proteins for Conformational Control

David Zanuy,[†] Ana I. Jiménez,[‡] Carlos Cativiela,[‡] Ruth Nussinov,*[,§,||] and Carlos Alemán*[,†]

Departament d'Enginyeria Química, ETSEIB, Universitat Politècnica de Catalunya, Diagonal 647, 08028 Barcelona, Spain, Departamento de Química Orgánica, ICMA, Universidad de Zaragoza−CSIC, 50009 Zaragoza, Spain, Basic Research Program, SAIC-Frederick, Inc. Center for Cancer Research Nanobiology Program, National Cancer Institute, Frederick, Maryland 21702, and Department of Human Genetics, Sackler Medical School, Tel Aviv University, Tel Aviv 69978, Israel

Received: August 4, 2006; In Final Form: November 20, 2006

A highly constrained amino acid has been introduced in the turn region of a β-helix to increase the conformational stability of the native fold for nanotechnological purposes. The influence of this specific amino acid replacement in the final organization of β-helix motifs has been evaluated by combining ab initio first-principles calculations on model systems and molecular dynamics simulations of entire peptide segments. The former methodology, which has been applied to a sequence containing three amino acids, has been used to develop adjusted templates. Calculations indicated that 1-amino-2,2-diphenylcyclopropanecarboxylic acid, a constrained cyclopropane analogue of phenylalanine, exhibits a strong tendency to form and promote folded conformations. On the other hand, molecular dynamics simulations are employed to probe the ability of such a synthetic amino acid to enhance the conformational stability of the β-helix motif, which is the first requirement for further protein nanoengineering. A highly regular segment from a naturally occurring β-helix protein was selected as a potential nanoconstruct module. Simulations of wild type and mutated segments revealed that the ability of the phenylalanine analogue to nucleate turn conformations enhances the conformational stability of the β-helix motif in isolated peptide segments.

Introduction

Redesigning protein structures into suitable biomaterials has been the focus of efforts by biologists and biophysicists in the last decades. Nonproteogenic amino acids with well-defined stereochemical and functional properties may enhance peptide and protein design.[1−5] They impose local restrictions on the chain by reducing its degrees of freedom, thus stabilizing secondary structures. However, the use of conformationally constrained amino acids for reengineering stable foldamers in order to enhance the formation of nanodevices is still incipient or even nonexistent.

Repeat proteins have recurrently been studied as well-suited candidates to become the scaffolds of new engineered nanoconstructs.[6] In this context, highly regular folded modules extracted from β-helix proteins could be selected as assembly modules. This β-helix motif is characterized by a series of progressive coils, each of which contributes to the three long β-sheets that form a triangular prism shape that comprises the fold.[7] The nanoconstruct "building blocks" will then be constituted by excised segments that presented a β-helix folding when part of the whole protein. The development of nanoconstructs from these modules first implies the stabilization of the desired fold motif out of its natural environment.[8] The first step to such a goal will comprise targeted replacement with conformationally restricted amino acids: the results presented in this work will demonstrate that these constrained amino acids are feasible candidates to stabilize the β-helix architecture and, therefore, to increase the population of properly folded states suitable of organizing into more complex nanostructures.

The β-helix main motif presents a high density of turns that connect each β-sheet segment. To increase the conformational stability of the turn conformations, a cyclopropane analogue of phenylalanine bearing two geminal phenyl substituents will be studied. This amino acid, 1-amino-2,2-diphenylcyclopropanecarboxylic acid (c_3Dip), is schematically depicted in Figure 1a. The strong stereochemical constraints of c_3Dip are induced by the cyclopropane moiety and by the interactions between the rigidly held aromatic side chains and the peptide backbone. This amino acid has been shown[9] to override the conformational propensities of proline and thus induce a double γ-turn (an incipient 2.2_7-helix) in a linear dipeptide in the crystalline state. Such a structural motif had been predicted but never characterized before in linear peptides based exclusively on proteinogenic amino acids. The high tendency of c_3Dip to adopt folded conformations has also been shown theoretically on a diamide derivative.[10]

Rigorous description of the conformational properties of any given protein segment would imply the exploration of the entire hypersurface of potential energy. In other words, the whole folding/unfolding equilibrium should be computed, which is still beyond the computational capabilities in systems the size of peptides and proteins.[11] Nonetheless, molecular dynamics (MD) simulations can be used to probe the feasibility of certain nanoconstructs by means of relative stability comparison.[12] If any previously selected building block must form assembled nanotubes, these constructions should be retained *in silico* under ideal conditions. At the same time, the information provided by these procedures can help to detect which are the most

* Corresponding authors. E-mail: carlos.aleman@upc.edu (C.A.); ruthn@ncifcrf.gov (R.N.).
[†] Universitat Politècnica de Catalunya.
[‡] Universidad de Zaragoza−CSIC.
[§] NCI.
[||] Tel Aviv University.

10.1021/jp065025k CCC: $37.00
Published on Web 03/08/2007

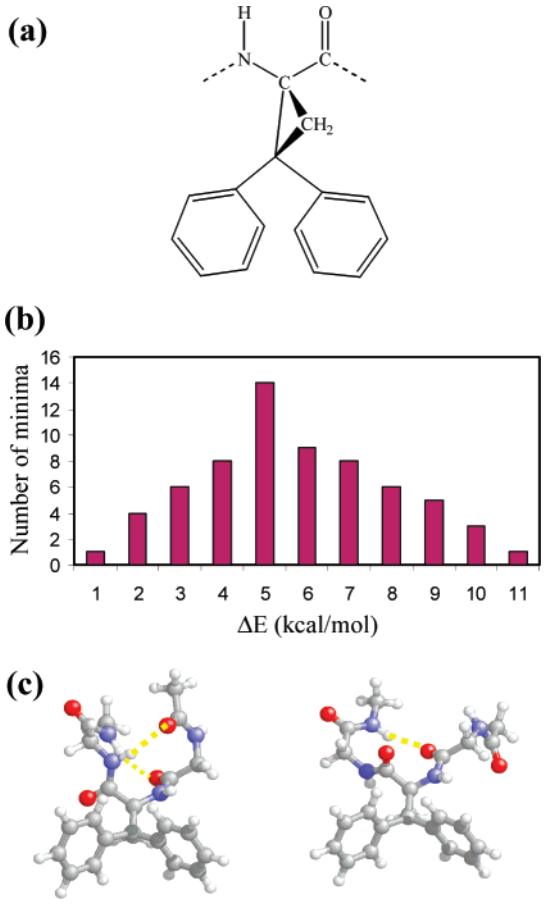

Figure 1. (a) Schematic representation of the molecular constitution of 1-amino-2,2-diphenylcyclopropanecarboxylic acid (L-c_3Dip). (b) Distribution of energies for the minimum energy structures calculated for Ac-Gly-L-c_3Dip-Gly-NHMe using quantum mechanical calculations at the HF/6-31G(d) level. (c) For the Ac-Gly-L-c_3Dip-Gly-NHMe tripeptide: (left) global minimum and (right) local minimum with a conformation very similar to that of Gly159-Ala160-Gly161 in krr1. Intramolecular hydrogen bonds are depicted using yellow dashed lines.

flexible parts of any given theoretical building block. Thus, in order to reduce the global conformational freedom of the selected block, these segments become preferred targets for amino acid replacement. Finally, even though the stability of the designed nanotube is not proved, those segments that are unsuitable can be rapidly discarded.[13]

Very recently, a segment obtained from *E. coli* galactoside acetyltransferase (Protein Databank (PDB) code krr1),[14] residues comprised between 131 and 165 ($krr1_{131-165}$), demonstrated to be an excellent candidate to form self-assembled nanotubes.[13] Its predicted native propensity to stabilize nanotube assemblies makes this segment a perfect candidate for target replacement with c_3Dip. The native conformation of the $krr1_{131-165}$ segment before association would not be the most populated in solution, which grants the necessity of the targeted replacement to enhance the weight of the desired fold.[8] It is worth noting that at this point of our research we only seek to study the conformational impact of inserting c_3Dip residue in the $krr1_{131-165}$ segment. However, in order to successfully promote the nanostructure formation it, would not sufficient to only enhance the stability of the desired conformation. Other important factors, such as the formation of aggregates instead of assemblies,[15−16] could negatively interfere with the formation of the nanoconstructs. Nonetheless, all these questions are beyond the scope of the current work and will be studied in the future.

In that context, we will demonstrate that synthetic residues are suitable candidates to stabilize β-helix motifs: the replacement of Ala160 by the c_3Dip enantiomer of the same configuration (L) enhanced the stability of the peptide segment in terms of reduction in the conformational flexibility. In $krr1_{131-165}$ the Ala residue is located at a turn region of the β-helix, where the β-sheet is interrupted and changes direction, and is involved in a β-turn (see the Supporting Information). Thus, the purpose of this residue replacement was to increase the stability in this region of the β-helix by introducing a constrained amino acid with a very high tendency to promote turn conformations.[9,10] It should be noted that Ala160 is flanked by the highly flexible Gly159 and Gly161, which would soften the strain introduced by c_3Dip. The work is divided in two parts. First, the intrinsic conformational properties of the peptide segment -Gly-L-c3Dip-Gly- are studied and compared with those of -Gly-Ala-Gly- using quantum mechanics calculations. Further, the target segment is introduced into $krr1_{131-165}$ and the effect on the conformational stability is assessed by means of molecular dynamics simulations.

Methods

All ab initio quantum mechanical calculations were performed using the Gaussian 03 computer program.[17] Full geometry optimizations were carried out at the Hartree−Fock (HF) level using a 6-31G(d) basis set.[18] Single point energy calculations were performed using HF/6-31G(d) geometries at the density functional theory (DFT) level with the following combination: Becke's three parameter hybrid functional (B3)[19] with the Lee, Yang, and Parr (LYP)[20] expression for the nonlocal correlation (B3LYP), completed with a 6-311++G(d,p)[21] basis set.

Three independent sets of molecular dynamics simulations were computed for each protein segment. Differences among sets relate to both heating and equilibration protocols, which is equivalent to generating uncorrelated trajectories. All the MD simulations were performed using the NAMD program.[22] Standard AMBER force-field parameters[23] were used for all the molecular species but L-c_3Dip, its parameters being those previously obtained to reproduce its specific conformational features.[24,25] The simulated protein fragment and its two replaced segments were placed in the center of a cubic simulation box of 56 Å axis length, filled with 5656 explicit water solvent molecules, which were represented using the TIP3 model.[26] Each system contained approximately 17 500 atoms including the solvent. Each simulated peptide was conveniently blocked at the N_t- and C_t-termini by an acetyl group and a methylamide group, respectively. The van der Waals interactions were calculated applying a spherical distance cutoff of 14 Å, and electrostatic interactions were computed without truncation via PME.[27] The real-space term was determined by the van der Waals cutoff (14 Å), while the reciprocal term was estimated by interpolation of the effective charge into a charge mesh with a 56-point grid. Periodic boundary conditions were applied by using the nearest image convention. All nonbonding atom pairs were updated every 25 steps, and the integration step was set to 2 fs. The SHAKE algorithm was applied to all bonds that contained hydrogen atoms.[28]

For each simulation, the solvent box was independently equilibrated with a combination of NVT−NPT short molecular dynamics rounds, freezing the protein segment during the process. All simulations were performed at 298 K using NPT conditions (pressure $\approx$1 atm) with the Berendsen weak coupling method.[29] An isothermal equilibration period of 0.5, 1, and 1.5 ns, respectively, was used for each simulation set, applying

TABLE 1: Categorization of the 64 Minima[a] Predicted for the Ac-Gly-L-c_3Dip-Gly-NHMe Tripeptide[b]

class[c]	min[d] (%)	subclass	min[e]	H-bonds[f]/conf[g]	ΔE[h]
III	5 (7.8%)	IIIa	4	C_7, C_7, $C_7/\gamma_D(4)$	0.8−2.1
		IIIb	1	C_7, C_7, $C_{10}/\gamma_D(1)$	2.0
II	21 (32.8%)	IIa	10	C_7, $C_7/\epsilon_D(2)$, $\alpha_L(1)$, $\gamma_D(7)$	2.6−5.5
		IIb	6	C_7, $C_{10}/\epsilon_D(1)$, $\alpha_L(4)$, $\epsilon_L(1)$	1.5−5.3
		IIc	3	C_7, $C_{11}/\alpha_L(1)$, $\gamma_D(2)$	0.9−2.4
		IId	1	C_7, $C_{13}/\gamma_D(1)$	3.3
		IIe	1	C_{10}, $C_{10}/\alpha_L(1)$	0.0
I	28 (43.7%)	Ia	14	$C_7/\epsilon_D(6)$, $\alpha_L(4)$, $\epsilon_L(2)$, $\gamma_D(2)$	2.9−8.3
		Ib	10	$C_{10}/\epsilon_D(3)$, $\alpha_L(3)$, $\epsilon_L(4)$	1.5−8.6
		Ic	2	$C_8/\epsilon_D(2)$	7.3−8.5
		Id	1	$C_{11}/\alpha_L(1)$	1.3
		Ie	1	$C_{13}/\epsilon_L(1)$	4.6
∅	10 (15.6%)			$-/\epsilon_D(2)$, $\alpha_L(1)$, $\epsilon_L(7)$	3.3−9.1

[a] Minima provided by ab initio HF/6-31G(d) calculations. [b] The minima have been classified in four classes depending on the number of intramolecular hydrogen bonds. Classes are divided in subclasses depending on the hydrogen bond type. For each subclass, the conformation of L-c_3Dip and the range of relative energies of the minima are specified. [c] Classes III, II, I, and ∅ correspond to structures containing 3, 2, 1, and 0 hydrogen bonds, respectively. [d] Number of minima and population of each class. [e] Number of minima of each subclass. [f] In the C_n notation, *n* indicates the number of atoms involved in the hydrogen-bonded ring. [g] See ref 8 for notation. The number of minima with a given conformation is indicated in parentheses. [h] In kcal/mol.

harmonic constraints to all the amide groups involved in the hydrogen bond formation of the last two sets, for the whole equilibration period. All those simulations were followed by 0.5 ns of isobaric equilibration, whereas harmonic constraints were slowly removed if present. This last step was the starting point for 10 ns trajectories, where coordinates were saved every 2 ps. In the next section we present the trajectories obtained using 1.5 ns of isothermal equilibration, a protocol that produced the lowest conformational fluctuations. The results provided by the rest of the trajectories are described in the Supporting Information.

Results and Discussion

As hinted above, reengineering protein modules for nanotechnology applications requires control over the conformational preferences of the selected monomer blocks, once they are extracted from the protein unity. The use of the accumulated organic chemistry background about synthetic amino acids with conformational constraints is an important tool for success in such chemical control. However, the experimental information available only involves either single amino acids or small peptides. Hence, organic chemistry information must be combined with theoretical approaches to predict the impact of inserting unnatural amino acids on the conformational properties of β-helix modules.

To analyze this question, the conformational properties of Ac-Gly-L-c_3Dip-Gly-NHMe, where Ac and NHMe refer to the acetyl and methylamide blocking groups, were first investigated using ab initio quantum mechanical calculations. A chain growth strategy generated 100 structures for this tripeptide, which were taken as starting points in geometry optimizations at the HF/6-31G(d) level. In this strategy we combined the minimum energy structures of the single residues, i.e., five and four minima for Ac-Gly-NHMe and Ac-L-c_3Dip-NHMe, respectively, to build up $5 \times 4 \times 5$ potential low-energy structures for the tripeptide. The calculations provided a total of 64 different minima with energies differing by 9.1 kcal/mol. The distribution of the energies associated with these minima fits a Gaussian function (Figure 1b), which is expected for the density of states provided by the rotational isomeric approximation with the assumption that the molecule is composed of *N* independent rotamers,[30] confirming the efficiency of the chain growth procedure. Using the absolute minimum conformation as reference, single point energy calculations at the B3LYP/6311++G(d,p) level were performed on those 17 structures that were unfavored by less than 3 kcal/mol. It is worth noting that energies computed at the latter level are in good agreement with those obtained at the HF/6-31(d) level (see the Supporting Information for details): Not only the absolute minimum corresponds to the same conformation but also most of the structures that were less favored with energies between 2 and 2.5 kcal/mol kept those differences beneath the 3 kcal/mol threshold with the DFT level.

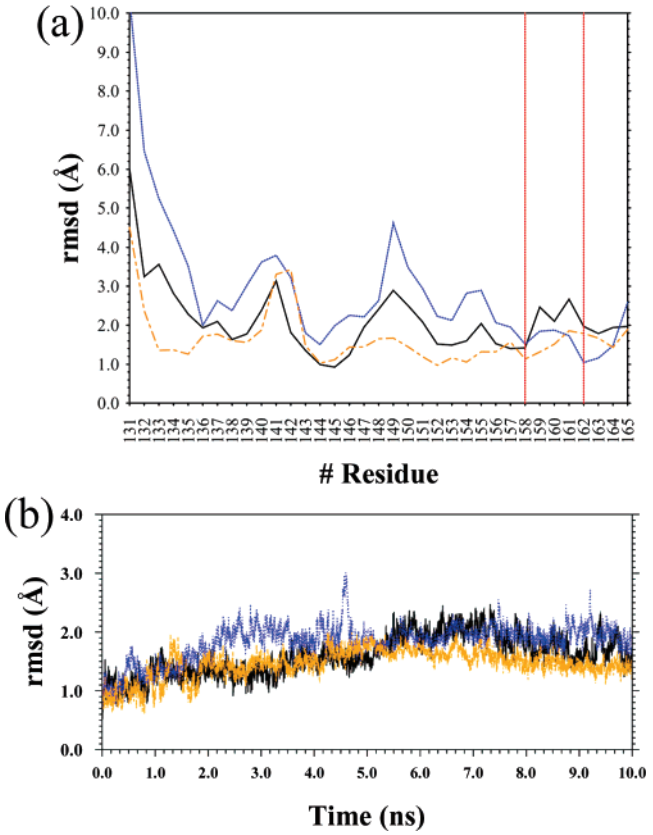

Figure 2. (a) Average rmsd for the 35 residues of the simulated systems and (b) temporal evolution of the rmsd calculated without considering the residues at the N_t-extreme: wild type (black), model I (orange), and model II (blue).

The minima of Ac-Gly-L-c_3Dip-Gly-NHMe were classified according to the number of intramolecular hydrogen bonds and the size of the *n*-membered ring defined by this interaction (C_n).

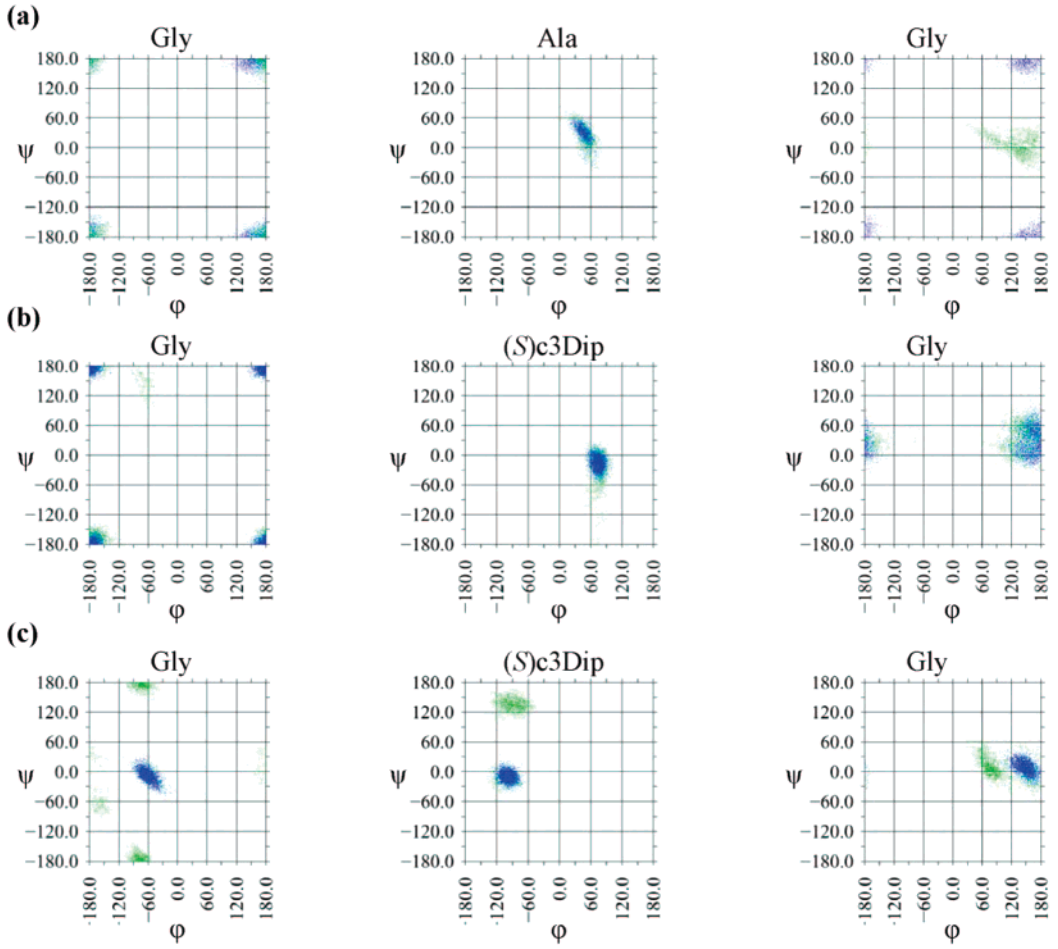

Figure 3. Accumulated Ramachandran plots through 10 ns of simulation corresponding to the segment Gly159-Xxx160-Gly161 for the wild type (a), model I (b), and model II (c). The accumulated (φ,ψ) pairs for the first and last 5 ns are depicted in green and blue, respectively.

For instance, C_7, C_{10}, and C_{13} correspond to the hydrogen-bonded rings characteristic of the γ-turn, β-turn, and α-helix conformations. Table 1 provides the distribution of the 64 minima in classes III, II, I, and ∅, which contain 3, 2, 1, and 0 hydrogen bonds, respectively. At the same time, each class is divided into subclasses depending on the hydrogen bond class. The conformational analysis is then focused on the central residue, since the terminal Gly residues are assumed to have their fold subordinated to the central residue one. For each class, the frequency of the different conformations adopted by L-c_3-Dip within the tripeptide is also displayed. Only four of the nine conformations identified on the Ramachandran map $E = E(\varphi,\psi)$ are observed for this residue, even though the neighboring glycines do not induce unfavorable steric clashes. According to the early shorthand notation for typical backbone folds,[31,32] the conformations allowed for L-c_3Dip are γ_D ($\varphi,\psi \approx 60°,-60°$), ϵ_D (180°,0°), α_L (−60°,−60°) and ϵ_L (0°,180°), with only γ_D, α_L, and ϵ_L being detected in low-energy structures of Ac-Gly-L-c_3Dip-Gly-NHMe.

Interestingly, the most populated is class I (44%) and, within it, conformations with a C_7 hydrogen bond. Moreover, 78% of the minima contain at least one C_7 or C_{10} hydrogen bond, indicating that L-c_3Dip exhibits a strong tendency to form and promote folded (γ- and β-turn) conformations, which is fully consistent with previous experimental and theoretical results.[9] The lowest energy conformation (Figure 1c, left) corresponds to two consecutive β-turns. Although not resembling the Gly-Ala-Gly motif in the crystallized β-helix, it was selected for subsequent molecular dynamics (MD) studies due to its high stability (Ala160c_3Dip-model I, see below); i.e., the next minimum is 0.9 kcal/mol higher in energy. Within the remaining 63 minima, one of those containing a single C_{10} (Figure 1c, right) is conformationally very close to the native Gly-Ala-Gly motif (dihedral angles are available in the Supporting Information). Since this conformation is only 2.9 kcal/mol less stable than the global minimum at both the HF/6-31G(d) and B3LYP/6-311++G(d,p) levels of theory, it was also chosen for targeted replacement in the β-helix architecture (Ala160c_3Dip-model II, see below).

As previously mentioned, the use of molecular dynamics simulations to establish absolute stabilities of the conformational motifs in protein segments of more than a dozen of residues is still beyond the scope of the current computational capabilities. However, it is possible to obtain qualitative and quantitative assessments of relative stabilities by systematic comparisons between different folded motifs and/or protein sequences. Hence, if under the same simulation conditions two proteins that only differ in one residue show different dynamic behaviors, it is possible to assess that the change in the stability of a particular folded motif is induced by such a replacement. In this context, independent MD simulations of the krr1$_{131-165}$ segment were performed in aqueous solution. The starting geometry was taken from PDB krr1; i.e., the native conformation of the krr1$_{131-165}$ segment was initially used for all the residues except in those positions where L-c3Dip was inserted, in which case the conformations derived from quantum mechanical calculations were used. Thus, three different starting points were used: the native conformation with the original sequence, named "wild

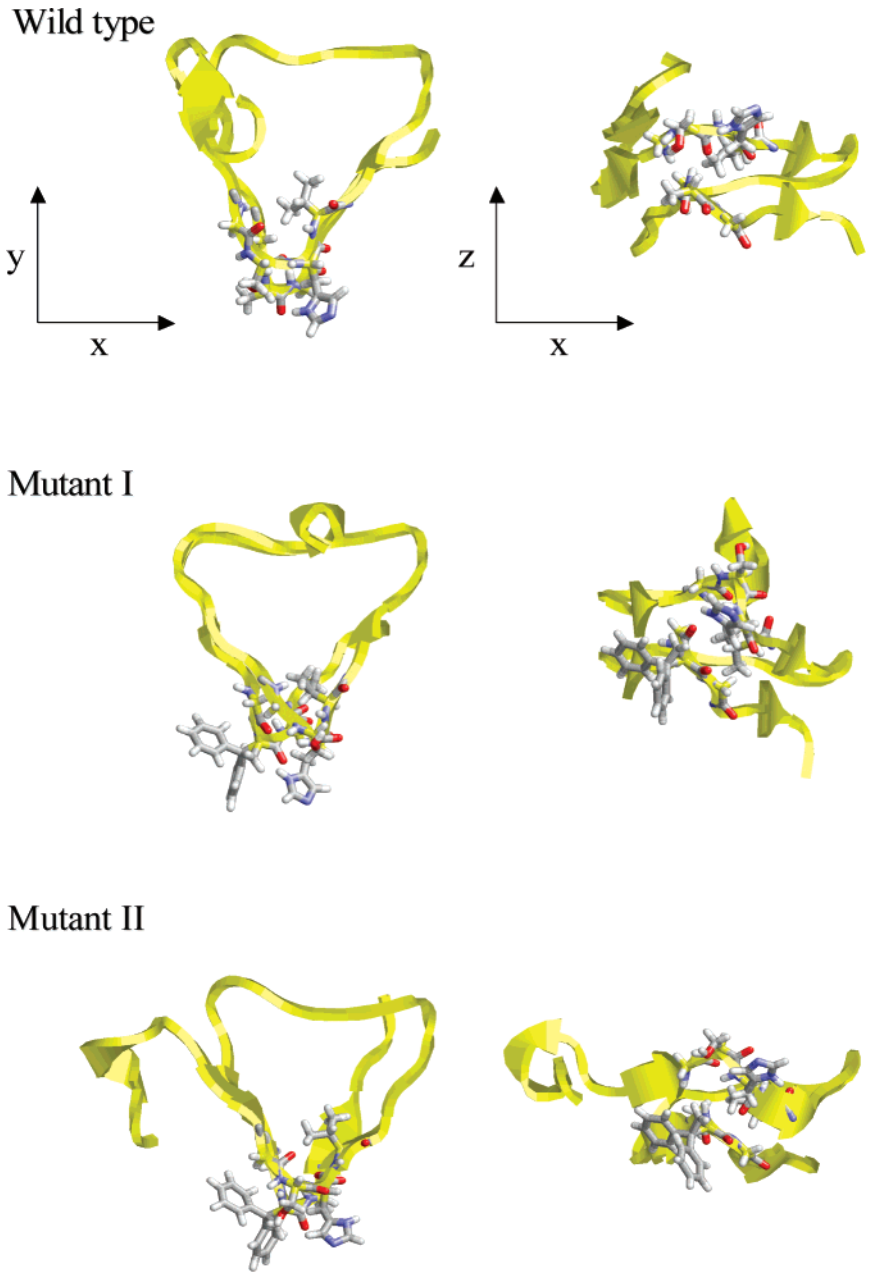

Figure 4. For the wild type, model I, and model II systems: left-handed β-helix structure obtained after 10 ns of simulation. The explicit atoms with the exception of those close to the loop under study are omitted for clarity.

type", and two more folds that presented L-c3Dip substituting Ala 160, as was already mentioned above. The latter peptides will only differ in the conformation adopted by the segment -Gly-L-c3Dip-Gly-, previously selected under the names "model I" (absolute minimum) and "model II" (minimum with the same geometry as to the native conformation).

Figure 2a, which presents the root-mean-square deviation (rmsd) of the 35 simulated residues averaged over the simulation (rmsd$^{\#}$), demonstrates that the wild type system retained the main features of the initial left-handed β-helix architecture. This is evidenced by the small root-mean-square-deviation (2.669 $\pm$ 0.993 Å) of the averaged (over the 10 ns trajectory) vs the PDB coordinates. It reveals as well, that there is only a significant distortion at the fraying end (residues 131−135). Recalculation of the temporal evolution of the rmsd without such residues of the N_t-extreme (Figure 2b) shows remarkably low conformational flexibility, with rmsd $\approx$ 2 Å during the last 5 ns of the trajectory. Thus, there is a remarkable ability to maintain the studied conformational motif, once it reaches a relaxed organization. This remaining conformation is not identical to that seen in the whole krr1 protein, since the shortened segment presents higher flexibility, to which the small peptide needs to dynamically readapt. The overall behavior observed in each set of simulations was analogous to that shown below, presenting between them only very small variations in the final reorganized conformation.

Figure 2 also compares both the rmsd$^{\#}$ and rmsd values calculated for the two substituted models and the wild type. The replaced segments present tail fraying at the N_t-terminus as well, an effect that arises from the omission of the rest of the protein. The rmsd without the unfolded N_t-extreme (residues 131−134 and 131−136 for models I and II, respectively) indicates that mutating Ala160 by L-c_3Dip enhances the stability of the β-helix motif (Figure 2b). This statement is inferred by the drastic reduction of the conformational flexibility especially in the mutated segments: the averaged rmsd of the Gly159-

Xxx160-Gly161 fragment is much smaller when Xxx = L-c_3-Dip (1.835 ± 0.822 Å and 1.564 ± 0.359 Å for models I and II, respectively) than in the wild type (Xxx = Ala, 2.578 ± 0.809 Å).

Analysis of the main chain dihedral angles indicates that the organization of the turn self-adapts toward accommodating the initial rigid motif to the peptide regular β-helix organization (Figure 3): the conformation adopted by the turn in each case tends to cluster in a restricted conformational space for the central residue, while the C_t-Gly buffers the geometric restraints imposed by the central residue throughout increasing its conformational flexibility. Thus, both modeled segments reveal the formation of specific conformational motifs that prevail up to the end of each simulation, either by following an analogous dynamic evolution to the one observed with the wild type sequence (in model I) or by relaxing the initial conformation and adjusting the new motif into the bend architecture (in the case of model II).

Therefore, the incorporation of L-c_3Dip synthetic residue in the substitution of Ala_{160} does not produce significant alterations in the structure of the turn once the peptide conformation is rearranged to fit the new residue. This is illustrated in Figure 4, which compares the β-helix conformation of the wild type with that of models I and II after 10 ns of MD simulation. As can be seen, the structural organization of the turn at the β-helix was fully preserved after replacing Ala160 by such a conformationally restrained amino acid. Thus, the only lack of conformational order is found at the N_t-extreme that, as was discussed above, unfolds in all cases. On the other side, the turn stabilization helps to improve the general stability of the helical conformational motif.

Conclusions

In this work, the use of conformationally restricted amino acids to stabilize natural conformational motifs has been evaluated by combining different standard computational methodologies. After selecting a peptide segment, isolated from a naturally occurring β-helix protein, a turn containing the sequence Gly-Ala-Gly was selected to insert L-c_3Dip. The substitution of Ala by L-c_3Dip determined the molecular constitution of the template that was used to perform a complete conformational search with quantum mechanical calculations. The novelty of our strategy was based on the development of adjusted small templates before using MD simulations. In other words, the final classical mechanics approach is only used with those conformations that are most suitable to fit in the originally selected turn. Then, the whole peptide is probed with the template replacing the native sequence, using the former optimized ab initio geometry as starting point in the latter segment.

Our promising results suggest new possibilities for enhancing the stability of complex organizations, like the β-helix fold, through selected targeted replacements by conformationally constrained nonproteinogenic amino acids. Furthermore, this work provides a computational strategy to examine the suitability of specific replacements on systems of high complexity. Thus, molecular systems that are not suitable to carry out systematic studies due to their excessive size can be explored by previous first-principles characterization of the potential substitution sites.

Acknowledgment. Computer resources were generously provided by the Barcelona Supercomputer Center (BSC) and the Centre de Supercomputació de Catalunya (CESCA). We acknowledge the National Cancer Institute for partial allocation of computing time and staff support at the Advanced Biomedical Computing Center of the Frederick Cancer Research and Development Center. Classical simulations were partially performed by utilizing the high-performance computational capabilities of the Biowulf PC/Linux cluster at the National Institutes of Health, Bethesda, MD (http://biowulf.nih.gov). D.Z. thanks the Ramon y Cajal program of the Spanish MEC for financial support. This project has been funded in whole or in part with federal funds from the National Cancer Institute, National Institutes of Health, under Contract No. N01-CO-12400. The content of this publication does not necessarily reflect the view of the policies of the Department of Health and Human Services, nor does mention of trade names, commercial products, or organizations imply endorsement by the U.S. Government. This research was supported [in part] by the Intramural Research Program of the NIH, National Cancer Institute, Center for Cancer Research.

Supporting Information Available: Figures showing the $krr1_{131-165}$ crystalline structure, fluctuations, and spatiotemporal evolution of backbone rmsd in MD series I and II, snapshots corresponding to the simulation of wild type model in MD series I, snapshots corresponding to the simulation of models I and II in MD series I, and tables showing the amino acid sequence of $krr1_{131-165}$, all minima found through a systematic conformational search at the HF/6-31G(d) level, comparison of the energy differences computed at the HF/6-31G(d) and B3LYP/6-311++G(d,p) levels, and conformational features of the Gly-Xxx-Gly loop. This material is available free of charge via the Internet at http://pubs.acs.org.

References and Notes

(1) Venkatraman, J.; Shankaramma, S. C.; Balaram, P. *Chem. Rev.* **2001**, *101*, 3131.

(2) Hill, D. J.; Mio, M. J.; Prince, R. B.; Hughes, T. S.; Moore, J. S. *Chem. Rev.* **2001**, *101*, 3893.

(3) Toniolo, C.; Crisma, M.; Formaggio, F.; Peggion, C. *Biopolymers (Pept. Sci.)* **2001**, *60*, 396.

(4) Cowell, S. M.; Lee, Y. S.; Cain, J. P.; Hruby, V. J. *Curr. Med. Chem.* **2004**, *11*, 2785.

(5) Wang, L.; Schultz, P. G. *Angew. Chem., Int. Ed.* **2005**, *44*, 34.

(6) Main, E. R. G.; Lowe, A. R.; Mochrie, S. G. J.; Jackson, S. E.; Regan, L. *Curr. Opin. Struct. Biol.* **2005**, *15*, 464.

(7) Jenkins, J.; Pickersgill, R. *Prog. Biophys. Mol. Biol.* **2001**, *77*, 111.

(8) Alemán, C.; Zanuy, D.; Jiménez, A. I.; Cativiela, C.; Haspel, N.; Zheng, J.; Casanovas, J.; Wolfson, H.; Nussinov, R. *Phys. Biol.* **2006**, *3*, S54.

(9) Jiménez, A. I.; Ballano, G.; Cativiela, C. *Angew. Chem., Int. Ed.* **2005**, *44*, 396.

(10) Casanovas, J.; Jiménez, A. I.; Cativiela, C.; Pérez, J. J.; Alemán, C. *J. Phys. Chem. B* **2006**, *110*, 5762.

(11) Searle, M. S.; Ciani, B. *Curr. Opin. Struct. Biol.* **2004**, *14*, 458.

(12) Zanuy, D.; Porat, Y.; Gazit, E.; Nussinov, R. *Structure* **2004**, *12*, 439.

(13) Haspel, N.; Zanuy, D.; Alemán, C.; Wolfson, H.; Nussinov, R. *Structure* **2006**, *14*, 1137.

(14) Wang, X. G.; Olsen, L. R.; Roderick, S. L. *Structure* **2002**, *10*, 581.

(15) Main, E. R. G.; Xiong, Y.; Cocco, M. J.; D'Andrea, L.; Regan, L. *Structure* **2003**, *11*, 497.

(16) Devi, V. S.; Binz, H. K.; Stumpp, M. T.; Plückthun, A.; Bosshard, H. R.; Jelesarov, I. *Protein Sci.* **2004**, *13*, 2864.

(17) Frisch, M. J.; Trucks, G. W.; Schlegel, H. B.; Scuseria, G. E.; Robb, M. A.; Cheeseman, J. R.; Montgomery, J. A., Jr.; Vreven, T.; Kudin, K. N.; Burant, J. C.; Millam, J. M.; Iyengar, S. S.; Tomasi, J.; Barone, V.; Mennucci, B.; Cossi, M.; Scalmani, G.; Rega, N.; Petersson, G. A.; Nakatsuji, H.; Hada, M.; Ehara, M.; Toyota, K.; Fukuda, R.; Hasegawa, J.; Ishida, M.; Nakajima, T.; Honda, Y.; Kitao, O.; Nakai, H.; Klene, M.; Li, X.; Knox, J. E.; Hratchian, H. P.; Cross, J. B.; Bakken, V.; Adamo, C.;

Jaramillo, J.; Gomperts, R.; Stratmann, R. E.; Yazyev, O.; Austin, A. J.; Cammi, R.; Pomelli, C.; Ochterski, J. W.; Ayala, P. Y.; Morokuma, K.; Voth, G. A.; Salvador, P.; Dannenberg, J. J.; Zakrzewski, V. G.; Dapprich, S.; Daniels, A. D.; Strain, M. C.; Farkas, O.; Malick, D. K.; Rabuck, A. D.; Raghavachari, K.; Foresman, J. B.; Ortiz, J. V.; Cui, Q.; Baboul, A. G.; Clifford, S.; Cioslowski, J.; Stefanov, B. B.; Liu, G.; Liashenko, A.; Piskorz, P.; Komaromi, I.; Martin, R. L.; Fox, D. J.; Keith, T.; Al-Laham, M. A.; Peng, C. Y.; Nanayakkara, A.; Challacombe, M.; Gill, P. M. W.; Johnson, B.; Chen, W.; Wong, M. W.; Gonzalez, C.; Pople, J. A. *Gaussian 03*, revision B02; Gaussian, Inc.: Pittsburgh, PA, 2003.

(18) Hariharan, P. C.; Pople, J. A. *Theor. Chim. Acta* **1973**, *28*, 213.

(19) Becke, A. D. *J. Chem. Phys.* **1993**, *98*, 1372.

(20) Lee, C.; Yang, W.; Parr, R. G. *Phys. Rev. B* **1993**, *37*, 785.

(21) Frich, M. J.; Pople, J. A.; Krishnam, R.; Binkley, J. S. *J. Chem. Phys.* **1984**, *80*, 3264.

(22) Kale, L.; Skeel, R.; Bhandarkar, M.; Brunner, R.; Gursoy, A.; Krawetz, N.; Phillips, J.; Shinozaki, A.; Varadarajan, K.; Schulten, K. *J. Comput. Phys.* **1999**, *151*, 283.

(23) Cornell, W. D.; Cieplak, P.; Bayly, C. I.; Gould, I. R.; Merz, K. M., Jr.; Ferguson, D. M.; Spellmeyer, D. C.; Fox, T.; Caldwell, J. W.; Kollman, P. A. *J. Am. Chem. Soc.* **1995**, *117*, 5179.

(24) Alemán, C.; Casanovas, J.; Galembeck, S. E. *Comput.-Aided Mol. Des.* **1998**, *12*, 259.

(25) Gomez-Catalán, J.; Alemán, C.; Pérez, J. J. *Theor. Chem. Acc.* **2000**, *103*, 380.

(26) Jorgensen, W. L.; Chandrasekhar, J.; Madura, J. D.; Impey, R. W.; Klein, M. L. *J. Chem. Phys.* **1983**, *79*, 926.

(27) Darden, T.; York, D.; Pedersen, L. *J. Chem. Phys.* **1993**, *98*, 10089.

(28) Ryckaert, J. P.; Ciccotti, G.; Berendsen, H. J. C. *J. Comput. Phys.* **1977**, *23*, 327.

(29) Berendsen, H. J. C.; Postma, J. P. M.; van Gunsteren, W. F.; DiNola, A.; Haak, J. R. *J. Chem. Phys.* **1984**, *81*, 3684.

(30) Flory, P. J. *Statistical Mechanics of Chain Molecules*; Interscience Publishers: New York, 1969.

(31) Perczel, A.; Angyin, J. G.; Kajtar, M.; Viviani, W.; Rivail, J. L.; Marcoccia, J. F.; Csizmadia, I. G. *J. Am. Chem. Soc.* **1991**, *113*, 6256.

(32) Perczel, A.; Jakli, I.; Csizmadia, I. G. *Chem.—Eur. J.* **2003**, *9*, 5332.